

Microwave Synthesis of AlFeCuCrNi /TiB₂ High-Entropy Alloy Matrix Composites

Lijuan Lan^a, Tianjiao Pu, Yingying Gu, Chengyan Zhu and Heguo Zhu

College of Materials Science and Engineering, Nanjing University of Science and Technology, Nanjing, 210094; P. R. China

Abstract. The Al-Fe-Cu-Cr-Ni-Ti-B system was microwaved to generate high entropy alloy matrix composites reinforced by TiB₂ particles. The micro structure and reaction process of the composites were observed and investigated by modern analysis methods, including X-ray diffraction (XRD), scanning electron microscopy (SEM), X-ray energy dispersive spectroscopy (EDS) and differential scanning calorimeter (DSC) analysis. The results show that AlFeCuCrNi /TiB₂ composites can be prepared by microwave heating method. The matrix structure was FCC, and the reinforcement TiB₂ showed regular geometric morphology in the matrix and evenly distributed in the matrix when the volume fraction of the reinforcement is 10%. When the volume fraction of the reinforcement increased to 15%, TiB₂ partially aggregates in the matrix, and the system activation energy was 195.69 kJ/mol.

1. Introduction

Conventional alloys usually have one or two elements as the main elements. To meet industrial requirements, researchers add appropriate amounts of other elements to improve the properties of the alloy [1]. In the 1990s, scholar Ye Junwei et al [2] from Taiwan first proposed the concept of multi-principal high-entropy alloy, which attracted attention from domestic and foreign scholars. The consist of multi-principal high-entropy alloy is at least five elements, each of them takes up a content, ranging from 5% to 35%. This kind of alloy's properties are determined by a variety of principal elements [3]. It is found that the microstructure of high-entropy alloys is not so complex as predicted by traditional alloy design concepts. Due to the high entropy effect, the structure of high-entropy alloys is mainly composed of a single BCC, FCC or HCP solid solution phase, and also shows high

strength, hardness, excellent wear resistance, corrosion resistance, low temperature resistance, high temperature oxidation resistance and temper softening resistance [4-6].

Mixed entropy [7] is an important thermodynamic feature of high-entropy alloys distinguished from traditional alloys. Gibbs Free Energy Law:

$$\Delta G = \Delta H - T\Delta S \quad (1)$$

(ΔG is the change of free energy, H is the mixed enthalpy, T is the thermodynamic temperature, and S is the mixed entropy). Although the high-entropy alloy has high mixed entropy, the free energy of the system can be reduced, and the intermetallic space is largely suppressed. The formation of the compound makes it easier for the alloy to form a solid solution rather than an intermetallic compound when solidified [8].

At present, domestic and foreign scholars are increasingly mature in the study of high-entropy alloys, and there is less progress in high-entropy alloy-based

^aCorresponding author: lan_lj@163.com;

composites. In this paper, the TiB₂ enhanced AlFeCuCrNi high-entropy alloy matrix composites prepared by microwave sintering were studied. The prepared samples were analyzed by X-ray diffraction (XRD) and scanning electron microscopy (SEM). The microstructures and distribution of different TiB₂ volume fractions were studied. The DSC curve at different heating rates was also tested, and the reaction kinetics was studied to determine the activation energy of the reaction.

2. Experimental

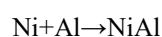
Ni powder (purity 99.8%), Fe powder (purity 99.4%), Cu powder (purity 99.5%), Al powder (purity 99.7%), Cr (purity 99.7%), Ti powder (purity 99.5%), B powder (purity 99.5%) were arranged according to a certain ratio. In the AlFeCuCrNi /TiB₂ high-entropy alloy matrix composite, the molar ratio is

Al:Fe:Cu:Cr:Ni=0.5:1:1.5:1:1, and the volume fraction of TiB₂ were respectively 10% and 15%. The sample is 30g per serving. The prepared powder was dried in a dry box. The powder mix was ball-milled in a stainless steel vacuum jar for 4 h and compacted under a pressure of 180 MPa into cylindrical specimens. Then, put the crucible with the pressure block into the microwave oven, closed the valve, vacuum, opened the control panel, set the heating and cooling program for microwave radiation, raised it to 1100 °C, and after cooling for 5 min, cool down to 100 °C with the furnace, took out the sample. The sample was ground, polished and mechanically polished and investigated by XRD and SEM equipped with an energy dispersive spectroscopy (EDS). Another dry powder of TiB₂ volume fraction of 15% was pressed into a thin sample, and 5-10 mg was placed in a differential scanning calorimeter to measure the DSC curve at different heating rates.

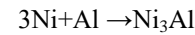
3. Results and discussion

3.1 Thermodynamic analysis of the reaction system

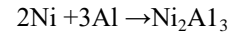
In the Al-Fe-Cu-Cr-Ni-Ti-B system, the main reactions that may occur are as follows:



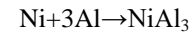
$$\Delta G_{\text{NiAl}, T}^{\theta} = -118407 + 4.10T \quad (2)$$



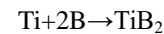
$$\Delta G_{\text{Ni}_3\text{Al}, T}^{\theta} = -153134 + 4.14T \quad (3)$$



$$\Delta G_{\text{Ni}_2\text{Al}_3, T}^{\theta} = -280420 + 8.15T \quad (4)$$



$$\Delta G_{\text{NiAl}_3, T}^{\theta} = -150624 + 4.17T \quad (5)$$



$$\Delta G_{\text{TiB}_2, T}^{\theta} = -281500 + 7.9T \quad (6)$$

From (1-1) to (1-5), it is clear that each equation is negative in the temperature range of the experiment. That is, from the thermodynamic point of view, each reaction may spontaneously proceed. Figure 1 is a graph showing the change of Gibbs free energy with temperature for NiAl, Ni₃Al, Ni₂Al₃, NiAl₃ and TiB₂. The figure shows that the Gibbs free energy of TiB₂ is the lowest, that is, the reaction is most likely to occur, so we can indicate that the reinforcement can be formed in the system.

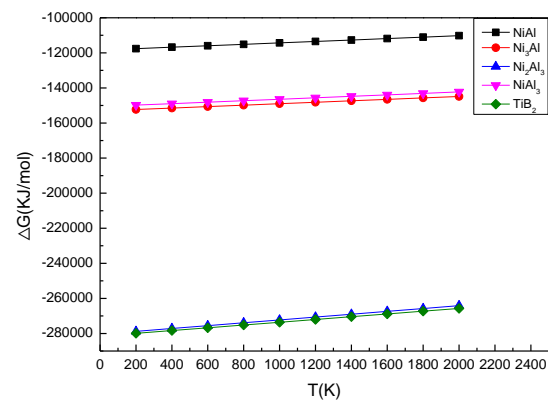


Fig.1 the change of Gibbs free energy with temperature for NiAl, Ni₃Al, Ni₂Al₃, NiAl₃ and TiB₂

3.2 SEM at different volume fractions and their corresponding XRD

Figures 2 and 3 respectively show SEM and XRD images with volume fractions of 10% and 15%. It can be seen from Fig. 2 that the bulk particles are distributed on the substrate with a scale of about 1 μm. The corresponding XRD indicates that the reaction product of the system

mainly has two phase structures, including the matrix phase and TiB₂. The matrix phase's structure is FCC. It can be seen from Fig. 3 that the TiB₂ particles are segregated and the dispersion is decreased, but the gap between the particles is reduced. It can be explained that the volume fraction is increased, and the heat of the thermal explosion reaction increases after the action of the microwave, which is favorable for diffusion and reduces the gap.

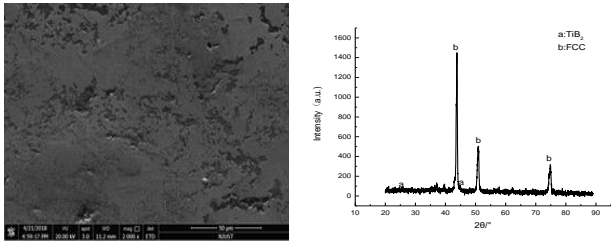


Fig.2 SEM and XRD images of the composites with volume fractions of 10%

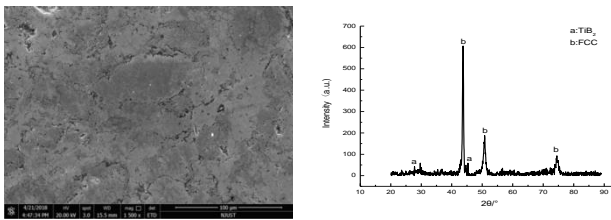


Fig.3 SEM and XRD images of the composites with volume fractions of 15%

3.3 DSC analysis at different heating rates (volume fraction 15%)

Fig. 4 is a DSC graph respectively showing heating rates of 10 K/min, 15 K/min, 20 K/min, and 25 K/min, when the volume fraction of the reinforcement is 15%. The figure indicates that there are obvious exothermic peaks at 800-900K under the four heating rates. With the increase of heating rate, the exothermic peak continuously moves back, the peak temperature is 835K, 842K, 844K, 859K, which is caused by the hysteresis of heat transfer. The higher the heating rate, the particle surface gets the energy of the reaction easier when the heating rate increases. Also, the transfer of heat takes time, which causes a temperature difference between the inside and outside of the particle, and the diffusion of the reactant takes time. Therefore, when the surface of the sample reaches the reaction temperature, the heat

accumulated in the sample is not enough to support the reaction due to the large temperature gradient. When the heat is transferred to the inside, the temperature of the furnace continues to rise, that is, the reaction temperature rises.

Calculated according to the kinetic model proposed by Kissinger [9]:

$$\frac{d(\ln \frac{\beta}{T_m^2})}{d(\frac{1}{T_m})} = -\frac{E_a}{R}$$

Where: β -temperature rate, K/min; E-phase change activation energy, kJ / mol; R-gas constant, J / mol K; T_m-peak temperature of the exothermic peak, K; C-constant. For the $\ln\beta/T^2 \sim 1/T$ plot, fit the line, as shown in Figure 5. Since the slope of the line is $-E_a/R$, the E_a value is obtained. By measuring the DSC curve at four heating rates, the reaction activation energy is 195.69 kJ/mol.

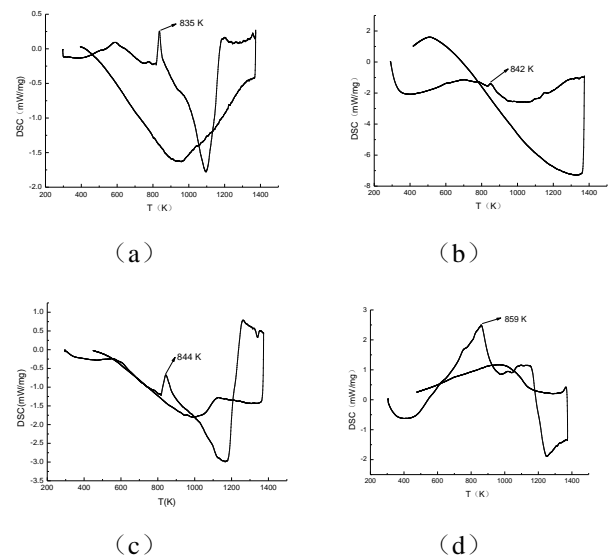


Fig.4 DSC curves of the powder mixture generated at different heating rates

(a) 10K/min (b) 15K/min (c) 20K/min (d) 25K/min

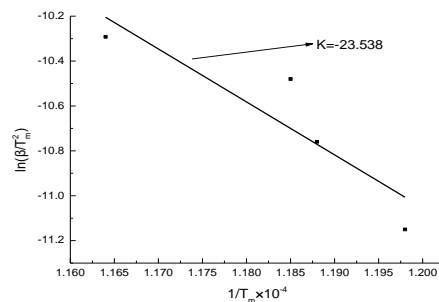


Fig.5 Plots of the $\ln(\beta/T_m^2) - 1/T_m$ of the for the

Al-Fe-Cu-Cr-Ni-Ti-B system

4. Conclusions

(1) AlFeCuCrNi /TiB₂ high-entropy alloy matrix composites can be prepared by microwave heating method. The matrix structure was FCC, and the reinforcement TiB₂ showed regular geometric morphology and dispersed in the matrix.

(2) When the volume fraction of the reinforcement is 10%, TiB₂ is more evenly distributed in the matrix. When the volume fraction of the reinforcement increases to 15%, TiB₂ partially aggregates in the matrix, and the system activation energy was 195.69 kJ/mol.

Acknowledgements

This work was supported by the National Natural Science Foundations of China (No.51571118 and 51371098); National undergraduate scientific research training project of China (201710288071); Natural Science Foundations of Jiangsu Province, China (No. BK20141308).

References

- [1] Greer A L. Nature. **366**. 303(1993).
- [2] Yeh J W, Chen S K, Lin S J, et al. Advanced Engineering Materials .**6**.299(2004).
- [3] Yeh J W, Chen S K. Metallurgical and Materials Transation. **A35**. 2533(2004).
- [4] Zhang Y, Zuo T T, Cheng Y, et al. Scientific Reports. **3**. 1355(2013).
- [5] Santodonato L J, Zhang Y. Nat Commun. **6**(2015).
- [6] Lim X. Nature. **533**. 306(2016).
- [7] Zhang D, Zhang N. Journal of Beijing Union University(Natural Sciences).**21**.4(2007).
- [8] Li Z L, Sun H F, Gao P, et al. Hot Working Technology.**39**.62(2010).
- [9] Zhang LC, Xu J, Eckert J. Journal of Applied Physical.**100**.(2006)